DEUTSCHES ELEKTRONEN – SYNCHROTRON

DESY 91-057
June 1991

Some Topics in *ep* Scattering at HERA: II. Parton Distributions in the Photon

H. Abramowicz
Institute of Experimental Physics, Warsaw University

K. Charchula, A. Levy
Deutsches Elektronen-Synchrotron DESY, Hamburg

M. Krawczyk
Institute of Theoretical Physics, Warsaw University

U. Maor
School of Physics, Tel-Aviv University

ISSN 0418-9833

NOTKESTRASSE 85 · D-2000 HAMBURG 52

To be sure that your preprints are promptly included in the
HIGH ENERGY PHYSICS INDEX,
send them to the following (if possible by air mail):

DESY
Bibliothek
Notkestrasse 85
D–2000 Hamburg 52
Germany

DESY 91-057
June 1991

ISSN 0418-9833

Some topics in *ep* scattering at HERA

II. Parton distributions in the photon

H.Abramowicz[3] , K.Charchula[1*], M.Krawczyk[4] , A.Levy[1†], and U.Maor[2]

1. Deutsches Elektronen-Synchrotron, DESY
2. School of Physics, Tel–Aviv University
3. Institute of Experimental Physics, Warsaw University
4. Institute of Theoretical Physics, Warsaw University

*On leave of absence from Institute of Experimental Physics, Warsaw University.
†On leave of absence from School of Physics, Tel-Aviv University.

II. Parton distributions in the photon

Abstract

The theoretical and experimental situation related to the photon structure function is reviewed. The existing parton distributions of the resolved photon are discussed in view of their need for the study of various processes at HERA.

Chapter 1

Introduction

First results from the electron–proton accelerator HERA will soon become available. The cross section for electron proton scattering is known to be dominated by low Q^2 photon exchange and, thus, the study of photoproduction on the nucleon with almost real photons with high production rates and the highest available energies will be possible. Since photoproduction processes are sensitive to the properties of the photon itself, the ep collider HERA can be thought of as an efficient tool to probe the structure of the photon as well as the structure of the proton.

The photon is a gauge particle mediating electromagnetic interactions. As such it couples to the elementary charged constituents of matter, like leptons and quarks, in a well defined way, which makes it a very good probing tool for the structure of more complicated objects like hadrons. This was used in the past to measure the parton distributions of the nucleon in deep inelastic scattering (DIS) processes. However, the point like nature of the photon, built in the Standard Model, has to be confronted with the fact that the photon may also exhibit properties similar to normal hadrons. The transition of the photon into hadronic systems is observed in photoproduction experiments as well as in e^+e^- interactions leading to two photon exchange. In the latter case, when one of the photons with very small virtuality interacts with the other one with high virtuality, the interaction can be thought of as a deep inelastic scattering of one photon on the other, in which case the situation is similar to the probing of a nucleon by a highly virtual photon. It is therefore natural to introduce the notion of the photon structure function in analogy to the well known nucleon case. For processes initiated by the photon, like heavy quark production, J/ψ production or deep inelastic QED Compton scattering, the photon structure function plays an important role, as the contribution of the resolved photon to the cross section may be substantial. Those processes can be studied in ep scattering, where the low Q^2 ep interactions can be interpreted in terms of γp scattering with a definite energy spectrum of real photons. In the equivalent photon approximation, photons with very small virtuality may be treated as real and their flux is described by the Weizsäcker–Williams formula [1,2].

The aim of this report is to introduce the reader to this interesting and increasingly important subject (see also earlier reviews on this subject [3,4,5]). The paper is divided into several parts. Chapter 2 is devoted to a detailed discussion of the structure of the real photon, its point–like and hadron–like components and its phenomenological and theoretical

interpretations. It contains a summary of the experimental information available on the photon structure function and a compilation of existing parametrizations with a particular emphasis on those which provide a parametrization of parton distributions in the photon, including a new parametrization based on all existing data. An important issue, which deserves a lot more attention, the one related to the structure of virtual photons, is treated briefly in the Chapter 3. A short review of processes relevant to ep scattering, in which the structure of the photon plays an important role and where one might even be tempted to measured it, follows in Chapter 4.

All along we have tried to keep the definitions very clear and we urge the reader to pay a special attention to it, as otherwise the picture may look very confusing. Unfortunately, this field has been plagued by different approaches and notations which have obscured our understanding of the actual physics.

Chapter 2

The structure of real photons.

2.1 Phenomenology.

2.1.1 The apparent structure of the photon

Hadrons are conceptually understood as extended confined systems of point–like constituents called partons which are associated with quarks and gluons. This substructure can be investigated through deep inelastic scattering experiments in which any of the electroweak vector bosons can serve as a probe whose interaction with the hadronic target is given as a non-coherent sum of its point–like interactions with the target partons. Indeed, our knowledge about the proton structure derives mostly from deep inelastic electron–proton, muon–proton and neutrino–proton scattering experiments.

In the classification of elementary particles, the photon plays the role of a gauge and point–like particle, mediating electromagnetic interactions through its coupling to the charge of matter. Yet, it is well known from soft, low energy γp interactions, that its behaviour can be similar to that of strongly interacting hadrons [6]. The properties of those interactions are well described by the Vector Dominance Model [7] (VDM), in which the photon turns first into a hadronic system with quantum numbers of a vector meson and then interacts with the target nucleon (see figure 1). The effective coupling of the photon to the vector–meson state can be determined experimentally. In more general models, such as GVDM [8] and EVDM [9], the interaction of the photon with a nucleon target is described by the contribution of an infinite sequence of vector mesons whose spectra and couplings (to the photon) depend on the specific model assumptions. In hard interactions, like heavy quark photoproduction, the photon may couple directly to the charged constituents of matter as shown in figure 2a – it behaves like a point–like particle. However, the photon may participate in such an interaction also through such processes as those depicted in figure 2b and figure 2c, where the photon fragments into quarks and gluons, which in turn participate in the hard process. The difference between the two cases is that in figure 2b the coupling of the photon to the initial quarks is point–like, as defined by the Standard Model, whereas in figure 2c the photon turns first into a vector meson state through a non–perturbative effective coupling. Whenever the photon turns into partons before interacting, be it through point–like couplings as shown in figure 2b or with hadron–like couplings as shown in figure 2c, it is called a **resolved** photon.

This behaviour of the interacting photon enables us to introduce and define a structure for the interacting photon.

2.1.2 Structure functions of the photon

In order to understand better the apparent structure of the photon, it is constructive to probe it in a similar way as that of the nucleon. The simplest solution is to use the photon itself as a probe and as a target. This procedure requires some caution as one has to be careful in distinguishing between the probing virtual photon and the target real photon.

The deep inelastic scattering (DIS) for $e\gamma$ interaction is depicted in figure 3a. To stress the analogy with the nucleon case, figure 3b shows the deep inelastic ep interaction. As in the case of a proton target one can define the structure functions of the photon through cross section considerations.

The following notation for the kinematical variables will be used:

- $p = (E, 0, 0, E)$ –four momentum of the incoming electron of energy E
- $p' = (E', 0, E'\sin\theta', E'\cos\theta')$ – four momentum of the outgoing electron of energy E' and polar angle θ' (the azimuthal symmetry is assumed explicitly)
- $k = (E_\gamma, 0, 0, -E_\gamma)$ – four momentum of the target photon
- $q = (p - p')$ –four momentum of the probing virtual photon

and the standard scaling variables are defined as follows:

$$\begin{aligned} Q^2 &= -(p-p')^2 = -q^2 > 0 \\ x &= \frac{Q^2}{2(q\cdot k)} \\ y &= \frac{q\cdot k}{p\cdot k} \\ z &= \frac{q\cdot k}{q\cdot p'}. \end{aligned} \tag{2.1}$$

The DIS cross section for an $e\gamma$ process

$$e + \gamma \rightarrow e + \text{hadrons} \tag{2.2}$$

with a real target photon, with only transverse polarization, can be described in terms of the absorption cross sections σ_{tt} and σ_{lt} for the transversely and longitudinally polarized virtual probe photon (with Hand's definition of the flux):

$$\frac{d\sigma}{dE'd\Omega'} = \frac{\alpha E'(y^2 - 2y + 2)}{2\pi^2 Q^2 y}(\sigma_{tt} + \varepsilon\sigma_{lt}) \tag{2.3}$$

where

$$\varepsilon = \frac{2(1-y)}{1+(1-y)^2} \tag{2.4}$$

If we introduce now the following notation

$$F_1^\gamma = \frac{Q^2}{4\pi^2\alpha}\frac{1}{2x}\sigma_{tt}$$

$$F_2^\gamma = \frac{Q^2}{4\pi^2\alpha}(\sigma_{tt}+\sigma_{lt})$$

the cross section for equation (2.3) can be rewritten in the following form:

$$\frac{d\sigma(e\gamma\to eX)}{dxdy} = \frac{4\pi\alpha^2 s}{Q^4}\{(1-y)F_2^\gamma + xy^2F_1^\gamma\} \tag{2.5}$$

which is to be compared to the proton case, where

$$\frac{d\sigma(ep\to eX)}{dxdy} = \frac{4\pi\alpha^2 s}{Q^4}\{(1-y)F_2^p + xy^2F_1^p\} \tag{2.6}$$

As one can see the similarity is complete. Therefore, F_i^γ from equation (2.5) can be treated as the structure functions of the target photon. The virtual probing photon is assumed to be a point-like object. The discussion of the nature of a virtual target photon will be given in chapter 3. As it happens, although a virtual photon may also develop a non-trivial structure, viewing it as a point-like object for the process (2.2) at large Q^2 is a very good approximation.

Presently, deep inelastic $e\gamma$ scattering is studied through e^+e^- interactions in which the two incoming leptons are scattered, i.e.

$$e^+ + e^- \to e^+ + e^- + \text{hadrons} \tag{2.7}$$

It proceeds via the reaction

$$\gamma^* + \gamma \to \text{hadrons} \tag{2.8}$$

where the probing photon γ^* is highly virtual and the target photon is almost real (see figure 3c). Due to a slight off-shellness, the target photons can have also a longitudinal polarization which in turn introduces an additional structure function F_3^γ [10] and the cross section becomes:

$$\frac{d\sigma}{dxdyd\phi/2\pi} = \frac{4\pi\alpha^2(kp)}{Q^4}[1+(1-y)^2]\{2xF_1^\gamma + \varepsilon(y)(F_2^\gamma - 2xF_1^\gamma) + \varepsilon(\zeta)\varepsilon(y)F_3^\gamma\cos 2\phi\} \tag{2.9}$$

where $\varepsilon(y)$ is the degree of polarization of the virtual probing photon q, and is given by equation (2.4), $\varepsilon(\zeta = E_\gamma/E)$ is the same quantity for the real target photon k, and ϕ is the angle between the scattering plane of the small angle $e^\pm$ (target photon polarization) and the larger angle one. In practice no measurements of F_3^γ have been performed so far. Experimentally one performs the so-called 'single tag' experiment, in which only one of the final state leptons is observed while the other one scatters in the beam pipe. In this way the 'target' photon is almost real and one can integrate over ϕ, and consequently the term containing F_3^γ can be dropped.

In this language, reaction (2.7) can be viewed as a two steps process. In the first step the target photons are radiated by one of the electrons and then they are probed in a deep inelastic scattering by highly virtual photons γ^* emitted by the second electron. In order to take into account the momentum spread of the target photons and their slight off-shellness one uses the equivalent photon approximation. In this approach, described by the Weizsäcker-Williams (WW) formula [1], the photons are assumed to be emitted real and their momentum spread is modified appropriately. The validity of this approach has been established by many checks [10]. The equivalent photon approximation allows to relate the e^+e^- reaction to the deep inelastic $e\gamma$ one in the following way:

$$d\sigma_{ee\to eeX} = d\sigma_{e\gamma\to eX}\cdot f_{\gamma/e} \tag{2.10}$$

where $f_{\gamma/e}$ is given by the WW formula,

$$f_{\gamma/e} = \{\frac{\alpha}{\pi z}[(z^2-2z+2)\ln\frac{E(1-z)\theta'_{max}}{m_e z} - (1+z)]\} \tag{2.11}$$

where z is defined by equation (2.1) and θ'_{max} is the limiting scattering angle of the tagged electron.

Thus, the differential cross section for single-tag events can be used to determine experimentally the photon structure functions defined in equation (2.6). The interesting aspect of the photon structure functions is that they can be confronted with the Quark Parton Model(QPM) and its QCD improvements. In what follows we shall concentrate on the discussion of the F_2 structure function. The F_1 structure function is related to F_2 through the Callan-Gross relation [11] and in case of the photon, especially because of the relatively low y involved experimentally, its contribution is less important.

2.1.3 The quark-parton description of the photon

For a nucleon target, the scaling properties observed for F_2^p were understood in terms of the Quark-Parton Model (QPM) and it became natural to view the proton as composed of free quarks. The deep inelastic interaction of a probe with the nucleon is described by an incoherent sum of elastic scattering of the probe on free spin 1/2 quarks. This approach leads to the identification of the $F_2^p(=2xF_1^p)$ structure function as a sum of the contributions of all quarks and antiquarks that build up the proton

$$F_2^p(x) = \sum_{i=1}^{2f} x\ e_i^2\ q_i(x) \tag{2.12}$$

where $q_i(x)$ describes, by definition, the probability of finding a particular type of quarks (antiquarks) in the proton, and xe_i^2 is the elementary "cross section" for the elastic scattering. In the QCD improved Parton Model, this relation still holds in the leading log approximation(LLA) with the quark densities acquiring a logarithmic Q^2 dependence which violates Bjorken scaling.

In contrast to the nucleon, for a photon target one can predict the structure function of the photon directly from the Parton Model. This is attained by performing a full calculation of the cross section $\gamma^*\gamma \to X$ to the lowest order in α, i.e. for the process

$$\gamma^* + \gamma \to q + \bar{q} \tag{2.13}$$

which is electromagnetic with known couplings. Note, however, that such an approach disregards possible contributions to the cross section coming from the "hadronic" component of the photon which was introduced intuitively in chapter 2.1.1 and will be further discussed in chapter 2.1.4.

In the framework of the Parton Model, the interaction depicted in figure 3a goes through a box diagram (see figure 4). The result of this calculation is (for massive quarks)

$$F_2^\gamma(x,Q^2) = \frac{N_c\alpha}{\pi}\sum_{i=1}^{f} x e_{q_i}^4 \{[x^2+(1-x)^2]\ln\frac{W^2}{m_{q_i}^2} + 8x(1-x) - 1\} \tag{2.14}$$

where $N_c = 3$ is the number of quark colours and W is the invariant mass of the hadronic final state (see figure 5). The relation $F_2^\gamma = 2xF_1^\gamma$ holds as in the case of the nucleon.

By analogy to the nucleon case, one could think of F_2^γ as the sum of momentum weighted densities of quarks "inside" the photon:

$$F_2^\gamma(x,Q^2) = \sum_{i=1}^{2f} x e_i^2 \; q_i^\gamma(x,Q^2) \tag{2.15}$$

with

$$q_i^\gamma(x,Q^2) = \frac{N_c\alpha}{2\pi} e_{q_i}^2 \{[x^2+(1-x)^2]\ln\frac{Q^2(1-x)}{m_{q_i}^2 x} + 8x(1-x) - 1\}. \tag{2.16}$$

Relation (2.15) defines, to lowest order, what is meant by quark distributions in the photon. A similar form holds for antiquarks, where one has:

$$\bar{q}_i^\gamma(x,Q^2) = q_i^\gamma(x,Q^2). \tag{2.17}$$

For quark distributions, the analogy to the nucleon case is not obvious because the quarks within a hadron probed by a virtual photon are free and on mass shell, while in the case of the photon, the quark which couples to the probe photon is an inner part of a diagram, i.e. a virtual quark. Fortunately, as it happens, at large Q^2 the dominant contribution to $q^\gamma(x,Q^2)$ is associated with the $\ln Q^2$ dependence. This contribution is induced by configurations in which the virtual photon couples to almost real quarks (provided x is not too close to 0 or 1) like in the case of hadrons. For this contribution, the variable x is indeed equal to the fraction of the photon momentum carried by the quark.

In the QPM the proton structure function F_2^p is expected to fulfill Bjorken scaling, while F_2^γ manifests strong scaling violation even without the presence of gluon bremsstrahlung. The introduction of gluon bremsstrahlung, responsible for the scaling violation observed in the nucleon case, does not change essentially the character of the Q^2 dependence of the F_2^γ obtained already in QPM (a $\ln\ln Q^2$ modification). Thus, contrary to the character of scaling violation in the nucleon case, which yields a negative contribution at large x and a positive one at low x, the scaling violation for the photon is positive in the whole x region (already at the Born level). The other important difference between F_2^p and F_2^γ is that, while counting rules predict a nucleon structure function which drops at large x, F_2^γ is large in the high x region (see figure 5).

Since the quark distributions in the photon could be calculated exactly in the Parton Model, and some of the QCD leading logarithmic corrections (the so–called asymptotic solution with a simple log Q^2 dependence) could also be evaluated, it was hoped that the structure function of the photon would be one of the cleanest tests of QCD, since not only the Q^2 dependence but also the absolute value of the structure function could be predicted in principle by the theory. Unfortunately, it turns out to be much more complicated, mainly because the nonperturbative nature of the hadronic component of the photon cannot be neglected in a consistent way.

2.1.4 The Altarelli–Parisi evolution equations for the photon

The corrections for the parton distributions within the photon due to perturbative QCD are induced by gluons that can be emitted and absorbed by the strongly interacting quarks. This implementation of perturbative QCD which leads to the QCD improved Parton Model can be carried out in three different theoretical methods:

1. The Operator Product Expansion (OPE) utilizing the renormalization group equations [12,13].
2. A diagramatic approach [14].
3. The modified Altarelli-Parisi [15](AP) evolution equations [16,17,18].

These different approaches have been shown to produce the same asymptotic results in the leading log approximation (LLA) and next to leading log approximation (NLLA), even though they differ in some of the details. We present here the AP approach which can be easily compared with the more familiar proton evolution equations.

In order to write the AP equations for the photon we define a variable t,

$$t \equiv \ln\frac{Q^2}{\Lambda^2}, \tag{2.18}$$

where we identify Λ with Λ_{QCD}, and denote by

$$h_{box}(x) = N_c e_q^2 \frac{\alpha}{2\pi}[x^2+(1-x)^2] \tag{2.19}$$

the splitting function of the photon to a quark which multiplies the $\ln Q^2$ from the box diagram (see eq. (2.16)). With these definitions, the AP equations for the parton distributions in the photon look as follows:

$$\begin{aligned}
\frac{\partial f_{q/\gamma}(x,t)}{\partial t} &= h_{box}(x) + \frac{\alpha_S(t)}{2\pi}\int_x^1 \frac{dx'}{x'}\{P_{qq}(\frac{x}{x'})f_{q/\gamma}(x',t) + P_{qG}(\frac{x}{x'})f_{G/\gamma}(x',t)\} \\
\frac{\partial f_{G/\gamma}(x,t)}{\partial t} &= \frac{\alpha_S(t)}{2\pi}\int_x^1 \frac{dx'}{x'}\{\sum_{q,\bar{q}} P_{Gq}(\frac{x}{x'})f_{q/\gamma}(x',t) + P_{GG}(\frac{x}{x'})f_{G/\gamma}(x',t)\}
\end{aligned} \tag{2.20}$$

where $f_{q/\gamma}$ and $f_{G/\gamma}$ denote quark (antiquark) and gluon densities in the photon respectively. In the LLA, the P_{ij} are the one loop splitting functions and the one loop strong coupling constant is

$$\alpha_s(t) = \frac{12\pi}{(33 - n_F)\ln\frac{Q^2}{\Lambda^2}} = \frac{1}{b\ln\frac{Q^2}{\Lambda^2}} \tag{2.21}$$

where n_F is the number of flavors participating in the evolution. In terms of the interaction of the virtual probing photon with a real target photon, the h_{box} term represents the contribution from the scattering off a quark of momentum x without gluon radiation. The gluon radiation is taken into account by the P_{qq} and P_{Gq} terms describing the splitting of a quark into a quark and a gluon. P_{qG} describes the splitting of a gluon into a $q\bar{q}$ pair and P_{GG} is induced by the triple gluon vertex (see figure 6).

It is very instructive to study the relative contribution of various terms responsible for the variation with Q^2 of the quark distributions in the photon and to compare the results with the QCD evolution in the nucleon case. The logarithmic derivative of F_2^p, $dF_2^p/d\ln Q^2$ as a function of x for the proton is shown for $Q^2 = 10$ GeV^2 in figure 7a. It shows the well known result that gluon radiation of quarks (described by the P_{qG} splitting function) gives the dominant contribution at small x and is responsible for the positive scaling violation observed at low x, while the radiation of quarks by quarks gives a negative contribution which determines the negative scaling violation at larger x, where it is the dominant contribution [1]. The same features remain true in the evolution of the photon structure function as shown in figure 7b. The gluons give a positive contribution at low x, while the quark radiation of quarks gives a negative contribution. However, there is a third term which contributes to the derivative of F_2^γ, that is photon radiation of quarks determined by h_{box}. As one can see, this term gives a positive contribution at all x values and becomes dominant at high Q^2 values in the region of intermediate x values (see figure 7c). The net effect of the three contributions responsible for the evolution of the photon structure function is that scaling violation is positive for all x values. It is also this h_{box} term that determines the shape of the photon structure function, peaking at large x. The fact that at large Q^2 this term determines the logarithmic derivative of F_2^γ, and that its contribution can be calculated without further assumptions led to the belief that one could perform a full calculation of F_2^γ and determine Λ_{QCD} very precisely. As can be inferred from figure 7c, the evolution of the photon structure function is dominated by the box point-like contribution, only for intermediate x values, even at $Q^2 = 100$ GeV^2. The low x and large x regions are still influenced by other contributions which depend on the normalization at lower Q^2 values, where the hadronic contribution could have been substantial. This seems to indicate that a simple calculation of F_2^γ based only on the box contribution is not justified and one has to try to perform either the exact calculation or to have a less ambitious approach, in which the measurement of the complete (finite by definition) F_2^γ at a given Q_0^2 is taken as an input for further QCD evolution to the desired Q^2 value. This latter approach is identical to the approach applied to the nucleon case. The theoretical problems which are encountered in various attempts to perform an exact calculation of F_2^γ will be described in chapter 2.2.

In case of the QCD evolution equations for the photon structure function, the h_{box} term introduces an inhomogeneity to all parton densities in the photon. This is different from

[1] The contribution may become positive at some low x, depending on the shape of the quark distributions, e.g. for the valence quark distributions in the proton.

the proton case where all equations are homogeneous. Indeed if we set $h_{box} = 0$, equations (2.20) are reduced to the known evolution equations for the nucleon. The solution for this set of equations is given by a superposition of the general solution of the corresponding set of homogeneous equations and a particular solution of the inhomogeneous one. If the inhomogeneous solution is assumed to be determined by the contribution of h_{box}, this solution will depend only on the known point-like couplings of the photon to quarks and quarks to gluons and that is why it has been often identified with the **point-like** contribution to the photon structure function. In this approach the homogeneous solution, which fulfills the hadron-like evolution of the AP equations, is assigned to the **hadron-like** contribution to the photon structure function. For that part of the overall solution, like in the nucleon case, some input information is needed, from which the QCD evolution can be computed. It contains that part of the photon interaction where the photon couples effectively to a mesonic system before interacting. A commonly used parametrization for such input may be provided by either VDM (see [5] for example) or the data itself. The reason to call the homogeneous solution hadron-like is due to the fact that its x and Q^2 dependence is expected to have the same features as those of the solution of the AP equations for the nucleon case.

To summarize, here are some important points relevant to the photon structure function:

- The photon structure function peaks at high x. This comes from the point-like contribution determined by the box diagram, already in QPM. QCD evolution does not change this general trend, but adds to it a contribution which peaks at small x (see figure 5), which is typical for the evolution of a hadronic state.

- The scaling violation of F_2^γ is profoundly different from that observed for a hadronic target such as the proton. $F_2^\gamma(x, Q^2)$ has a logarithmic positive scaling violation ($\sim \ln Q^2$) for all x values. This is true in QPM and remains so in the framework of QCD. For the nucleon, Bjorken scaling is the signature of the Parton Model and the logarithmic scaling violation ($\sim \ln\ln Q^2$) necessitates the introduction of the QCD improved Parton Model. For the photon case the difference between the Parton Model and its QCD improvement is not fundamental but quantitative.

- Contrary to the nucleon case, where the parton distributions are constrained by sum-rules valid up to higher order corrections, there are no such sum rules for the photon case. This is probably due to the complicated nature of the photon being either a point-like particle or a particle with an apparent structure, which is reflected in that F_2^γ is of the order of the electromagnetic coupling α.

- As is known from the nucleon case the hadron-like contribution varies very slowly with Q^2, therefore it is expected that in the high Q^2 limit the point-like contribution will dominate over the hadron-like contribution. This observation, made first by Witten [12], means that at large Q^2, F_2^γ can be fully determined in perturbative QCD. Moreover, since the normalization of F_2^γ depends on $1/\alpha_S$, and thus on the QCD scale parameter Λ, it was hoped that the study of the F_2^γ could provide a direct determination of Λ. Unfortunately, due to many theoretical difficulties encountered in the calculation of F_2^γ, (to be discussed in the next chapter), the actual attempts to measure Λ through the study of F_2^γ have attained only a very limited success [19,3,4].

2.1.5 The role of the photon structure in photon induced reactions

Hard processes which occur in high energy hadron–hadron interactions are characterized by large momentum transfers or by the production of large invariant masses. Such processes are in general correctly described by the QCD improved Parton Model. In this framework, the factorization theorem allows to factorize the hard (lowest order) subprocess and the densities of partons initiating the subprocess. A typical example of such a hard process is provided by the inclusive production of a heavy quark q_H in two hadron interaction, depicted in figure 8,

$$A + B \rightarrow q_H + X \tag{2.22}$$

for which the cross section is given by

$$\sigma_{AB\rightarrow q_H X} = f_{a/A}(x_a, \cdots) \otimes \hat{\sigma}_{ab}(\hat{s}, x_a, x_b, \cdots) \otimes f_{b/B}(x_b, \cdots). \tag{2.23}$$

This is a factorized convolution of the scaling violating parton distributions $f_{a/A}$ and $f_{b/B}$ with the hard subprocess $\hat{\sigma}$. The energy square of the partonic center of mass system is denoted by $\hat{s}$, while x_a and x_b are the momentum fraction of the parent hadrons A and B carried out by partons a and b respectively. The scale at which each of the convoluted terms is to be evaluated is not specified in equation (2.23). In any case the scale should correspond to the hardness of the subprocess (determined for instance by p_T^2). Let us consider that one of the interacting particles is a photon:

$$\gamma + B \rightarrow q_H + X \tag{2.24}$$

The photon can participate directly in the hard subprocess, playing the role of a parton (see figure 9a). The appropriate cross section is given by

$$\sigma_{\gamma B\rightarrow q_H X} = \hat{\sigma}_{\gamma b}(\hat{s}, x_\gamma, x_b, \cdots) \otimes f_{b/B}(x_b, \cdots) \tag{2.25}$$

This is a direct interaction of the photon with parton b of particle B in the hard reaction (2.24) and x_γ is equal to 1. This is the so called **direct photon** interaction. However, it may well happen that the photon will not participate directly in the hard subprocess, but through a parton associated with its structure. In this case the inclusive cross section for (2.24) is given by

$$\sigma_{\gamma B\rightarrow q_H X} = f_{a/\gamma}(x_a, \cdots) \otimes \hat{\sigma}_{ab}(\hat{s}, x_a, x_b, \cdots) \otimes f_{b/B}(x_b, \cdots) \tag{2.26}$$

where $f_{a/\gamma}$ is the distribution function of parton a in the photon, related directly to F_2^γ discussed in the previous section (see figure 9b). This corresponds to the interaction of the **resolved photon** as shown in figure 2b and figure 2c. The cross section for reaction (2.24) is given, thus, by the sum of the partial cross sections (2.25) and (2.26).

For the sake of clarity and to avoid any confusion we summarize the definitions:

- When the photon participates directly in the hard subprocess its contribution is called direct and the hard photon couples to a charged parton through a point–like QED coupling.
- When the photon participates in the hard subprocess through one of its own partons, its contribution is called that of the resolved photon.

We note that the resolved photon can couple to its own partons either through point–like couplings or through hadron–like couplings, therefore both the point–like and the hadron–like sectors have to be included in the calculation. Alternatively, one may use an empirical knowledge of the photon structure function where no distinction between the two sectors is needed.

Those interesting aspects of the photon behaviour in hard interactions can be studied in high energy photoproduction processes. The best available "source" of high energy photons are the ep reactions, where the interacting photons are emitted by electrons. These photons are off–mass shell, but since the ep cross section is dominated by $Q^2 \simeq 0$, the virtuality of the photon on the average is very small and the equivalent photon approximation [1,2,10] in which the photons are treated as real (with a WW energy spectrum) is appropriate [20]. This is depicted in figure 10.

A nice example of these considerations is given by the analysis of two–jets production in very high energy ep interactions. This reaction has been analyzed in detail by Drees and Godbole [21] and is shown schematically in figure 11. The differential cross section is given by

$$\frac{d\sigma}{dp_T} = 2p_T \int_{\frac{4p_T^2}{s}}^1 dz f_{\gamma/e}(E,z) \int_{\frac{4p_T^2}{zs}}^1 dx_a \int_{\frac{4p_T^2}{x_a zs}}^1 dx_b f_{q/p}(x_a, \tilde{Q}_2) f_{b/\gamma}(x_b, \tilde{Q}^2) \frac{d\hat{\sigma}}{dp_T^2}(\hat{s}, \hat{t}, \hat{u}) \tag{2.27}$$

where s is the squared center of mass energy of the ep system, $\hat{s} = zs$ is the center of mass energy squared of the $\gamma^* p$ system, and $\hat{s} = x_a x_b s$ is that of the parton-parton system. The function $f_{\gamma/e}$ is the luminosity factor for the flux of interacting photons originating from the electron beam. The variable $\tilde{Q}^2$ denotes the scale of the hard interaction and should not be mistaken with the absolute value of the squared four–momentum transfer Q^2 from the electron to the nucleon system which determines the virtuality of the photon (which in this case is close to 0). As already mentioned earlier, there is no prescription as to what should be used for $\tilde{Q}^2$, but $\tilde{Q}^2 = p_T^2$ seems to reproduce well the $Sp\bar{p}S$ two jets data [22]. In the reaction described by the cross section above, the photon can interact either directly or through its own partons and all possible contributions have to be included. In case of the direct photon contribution the following holds:

$$f_{b/\gamma}(x_b, Q^2) = f_{\gamma/\gamma} = \delta(1 - x_b).$$

The interesting observation is that the contribution of the resolved photon to the interaction has a relatively clear signature, both due to kinematical considerations and to the expected presence of a soft spectator jet associated with the initial photon. Thus, this reaction may be used for further studies of $f_{b/\gamma}$ and F_2^γ.

2.2 Theoretical problems in the calculation of F_2^γ

Most of the important features concerning the photon structure, which may be relevant for practical use have already been presented. This chapter will be more technical. It is intended to clarify and summarize the theoretical situation concerning the structure function of a real photon, which is otherwise pretty confusing, especially for a reader inexperienced in this domain. It is not essential for a practical knowledge and those who are interested in practical applications can safely skip this chapter.

2.2.1 The Parton Model approach

As discussed in the previous chapter, F_2^γ can be calculated in the Quark Parton Model from the box diagram shown in figure 4. For the sake of completeness we repeat below the basic formula for the case of massive quarks:

$$F_2^\gamma(x,Q^2) = \frac{N_c\alpha}{\pi}\sum_i x e_{q_i}^4 \{[x^2+(1-x)^2]\ln\frac{W^2}{m_{q_i}^2} + 8x(1-x) - 1\}, \tag{2.28}$$

where W^2 and Q^2 are related through the formula

$$W^2 = Q^2\frac{1-x}{x}. \tag{2.29}$$

It is worth to notice that this formula can not be applied in the case of massless quarks, an approach used in the application of the QCD improved Parton Model. For massless quarks some regularization is needed, like the dimensional regularization [23] followed by a renormalization procedure , in order to obtain a finite result for F_2^γ. As a result, the predictions of the Parton Model will depend on regularization and renormalization schemes(!). Fortunately, these difficulties do not apply to the dominant term proportional to $\ln Q^2$ which does not depend on this arbitrary choice. The other (constant) terms are not universal. Therefore in many application the constant terms are neglected, and the following approximation is used:

$$q_{i,PM}^\gamma(x,Q^2) = \frac{N_c\alpha}{2\pi}e_{q_i}^2\,[x^2+(1-x)^2]\ln\frac{Q^2}{\Lambda^2}. \tag{2.30}$$

It is obvious that this formula does not approximate properly the full Parton Model result for x close to 0 and 1 (see formula (2.28) and figure 5). Thus, this formula can be used in the region of large Q^2 and x far from both limits. Its advantage lies in that it can be interpreted in terms of free quarks and, moreover, it has the structure of a leading logarithm (in Q^2). It is important to note that the parameter Λ in the above formula is in principle an arbitrary scale parameter which can be put equal to Λ_{QCD} from hadronic processes although there are no deeper arguments for doing so [24].

2.2.2 QCD in leading log approximation (LLA)

The AP equations for the evolution of the photon structure function in the LLA have been presented in chapter 2.1.4 where we have also associated the point–like and hadron–like sectors of the real target photon with the nonhomogeneous and homogeneous terms of the AP solution.

For a further discussion it is useful to introduce the moments of the functions appearing in the evolution equations. Defining the $n-th$ moment of a function f as

$$f^n = \int_0^1 x^{n-1}f(x)dx \tag{2.31}$$

we may rewrite equations (2.20) in the following form

$$\frac{\partial f_{q/\gamma}^n}{\partial t} = h_{box}^n + \frac{\alpha_S(t)}{2\pi}\{P_{qq}^n f_{q/\gamma}^n + P_{qG}^n f_{G/\gamma}^n\}$$

$$\frac{\partial f_{G/\gamma}^n}{\partial t} = \frac{\alpha_S(t)}{2\pi}\{\sum_{q,\bar q} P_{Gq}^n f_{q/\gamma}^n + P_{GG}^n f_{G/\gamma}^n\} \tag{2.32}$$

where the notation is the same as for equations (2.20) and, of course, the same equation as for quarks holds for the antiquarks. We obtain again an inhomogeneous set of equations. Thus, the solution of these equations is a superposition of a general solution of the homogeneous set and a particular solution of the inhomogeneous one. For the sake of simplicity only the non–singlet case will be discussed below, however the discussion can be easily extended to the singlet parton densities. In the non–singlet case, the gluons do not contribute and the set of equations (2.32) is reduced to only one inhomogeneous equation of the form:

$$\frac{\partial f_{q/\gamma}^n}{\partial t} = h_{box}^n + \frac{\alpha_S(t)}{2\pi}\{P_{qq}^n f_{q/\gamma}^n\} \tag{2.33}$$

In the LLA, the general solutions of the evolution equations for the non–singlet quark distribution in the hadronic case [24] is given by

$$f^n(Q^2) = [\frac{\alpha_s(Q^2)}{\alpha_s(Q_0^2)}]^{-d_{qq}^n} f^n(Q_0^2) \tag{2.34}$$

in which

$$d_{qq}^n = \frac{P_{qq}^n}{(2\pi b)} = \frac{\gamma_{qq}^n}{b} \tag{2.35}$$

where γ_{qq}^n is the anomalous dimension and b is defined by (2.21). The same form as in formula (2.34) holds for the general solution of the homogeneous equation for the non–singlet quark distributions of the photon. We will denote by $f_\gamma(x,Q^2)$ the non–singlet quark distribution and its moment by $f_\gamma^n(Q^2)$. The d_{qq}^n coefficient is known to be negative for n bigger than 1, and, thus, one might expect that the hadronic contribution (given by (2.34)) becomes less important with increasing Q^2.

For a particular solution of the inhomogeneous part, one can assume in LLA a factorized form with a simple $\ln Q^2$ dependence (as in the Parton Model result):

$$f_\gamma(x,Q^2)|_{asymp} = \frac{4\pi}{\alpha_s(Q^2)}A(x) \tag{2.36}$$

The function $A(x)$ can be calculated from the evolution equation (see [19] and [3] for details). Note that the above formula retains its structure also for the moments:

$$f_\gamma^n(Q^2)|_{asymp} = \frac{4\pi}{\alpha_s(Q^2)}A^n \tag{2.37}$$

with

$$A^n = \frac{a^n}{(1-d_{qq}^n)}, \tag{2.38}$$

and

$$a^n = \frac{\alpha}{4\pi}e_q^2 d_{q\gamma}^n \tag{2.39}$$

The coefficient $d_{q\gamma}^n$ is proportional to the one loop anomalous dimension $\gamma_{q\gamma}^n$ corresponding to the transition $\gamma - q$ and is equal to

$$d_{q\gamma}^n = \frac{P_{q\gamma}^n}{2\pi b} = \frac{\gamma_{q\gamma}^n}{b} \tag{2.40}$$

with $P^n_{q\gamma}$ being the n-th moment of $N_c[x^2+(1-x)^2]$.

Equation (2.36) can be interpreted as the result of the box diagram (equation (2.30)) renormalized by QCD corrections. It is customary to call this solution the **asymptotic point–like** solution.

By adding this solution to the homogeneous one, we obtain

$$f^n_\gamma(Q^2) = \frac{4\pi}{\alpha_s(Q^2)}A^n + (\frac{\alpha_s(Q^2)}{\alpha_s(Q^2_0)})^{-d^n_{qq}}\tilde{f}^n_\gamma(Q^2_0) \tag{2.41}$$

where the boundary function $\tilde{f}^n_\gamma$ is related to the quark distribution in the photon at an arbitrary scale Q^2_0

$$f^n_\gamma(Q^2_0) = \frac{4\pi}{\alpha_s(Q^2_0)}A^n + \tilde{f}^n_\gamma(Q^2_0). \tag{2.42}$$

This leads to the final general form of the solutions of equation (2.33):

$$f^n_\gamma(Q^2) = \frac{4\pi}{\alpha_s(Q^2)}[1-(\frac{\alpha_s(Q^2)}{\alpha_s(Q^2_0)})^{1-d^n_{qq}}]A^n + (\frac{\alpha_s(Q^2)}{\alpha_s(Q^2_0)})^{-d^n_{qq}}f^n_\gamma(Q^2_0). \tag{2.43}$$

Note that this solution of the evolution equation given by equation (2.43) contains terms which have different powers of $\ln Q^2$. This mixed character of the solution is due to the inhomogeneous term, present in equation (2.32).

If, in formula (2.43), terms less dominant in Q^2 are neglected, one obtains the asymptotic result given by equation (2.38). Since this contribution is completely calculable in QCD, there was hope that the structure function of the photon would be a unique test of QCD. If one accepts the asymptotic solution as relevant also at some finite large Q^2, then QCD predicts scaling violation proportional to $\ln(Q^2/\Lambda^2_{QCD})$ and, since the normalization of the photon structure function is known, the measurement of F^γ_2 at large Q^2 allows to determine the scale Λ_{QCD}. In other words one could say that in the LLA the QCD prediction for F^γ_2 has only one free parameter: Λ_{QCD}. It should be noted, though, that since the relative importance of various terms in eq. (2.43) was evaluated by comparing the moments integrated over x, it is not obvious whether the same arguments can be used in the x–space.

The function $A(x)$ for the non–singlet and singlet case as well as the individual quark and gluon distributions can be obtained by inverting the moments. Unfortunately, $A(x)$ for the singlet case happens to be singular at small x, for $x \to 0$, $A(x) \sim x^{-1.6}$. Thus, from a practical point of view the asymptotic solution obtained in LLA cannot be applied at very small x values, while the full solution given by equation (2.43) has a regular behaviour at small x. The term which regularizes the singularity of the asymptotic solution is the second term multiplying A^n. Although this term is less important for larger Q^2 than the asymptotic term, its role is to cancel the singularity at small x, which is built into the asymptotic part. It is important to retrace the origin of this regularizing term present in the full solution. It comes from the boundary condition (2.42) imposed on the full solution (see eq. (2.34)), and is related to the hadronic solution of the homogeneous part of equation (2.32) [25]. On the other hand, since this term is fully calculable in QCD, one can think of it as the point–like non leading term; however, originally it belongs to the hadronic solution (the second term in eq. (2.41)).

To conclude, the singularity problem encountered in the asymptotic prediction for $f_{q/\gamma}$ and, thus, F^γ_2 can be traced back to the hadronic contribution to the full solution of the AP equations. Regardless of the interpretation, the solution to the singularity problem requires some phenomenological handling of the hadron–like sector. The net result is that the sensitivity to Λ_{QCD} is lost, even though the LLA analysis can reproduce the data well.

2.2.3 QCD in next to leading log approximation (NLLA)

Before the origin of the singularity encountered in the LLA analysis of the photon structure function was well understood, it was hoped that the NLLA calculation could be of some help. In NLLA, both the splitting functions and the strong coupling constant in the AP equations have to be modified by second order corrections:

$$P^n = P^n_0 + \frac{\alpha_S}{2\pi}P^n_1 + \cdots \tag{2.44}$$

$$h^n_{box} = h^n_0 + \frac{\alpha_S}{2\pi}h^n_1 + \cdots \tag{2.45}$$

$$\alpha_S = 4\pi\{(11-\frac{2n_F}{3})\ln\frac{Q^2}{\Lambda^2} + \frac{102-\frac{38n_F}{3}}{11-\frac{2n_F}{3}}\ln(\ln\frac{Q^2}{\Lambda^2}) + \cdots\}^{-1} \tag{2.46}$$

where the 0 subscript stands for P^n and for h^n used in the LLA. In the NLLA, P^n_1, h^n_1, Λ and the results of the AP equations depend on the renormalization scheme. The relation between F^γ_2 and the parton distributions is scheme dependent and equation (2.15) is assumed to hold only in the so called DIS scheme. The structure function F^γ_2 itself, as a measurable physical quantity, should not depend on the scheme, as in the nucleon case.

In the NLLA, as in the LLA case, we shall concentrate again only on the non–singlet case, although the same argumentation holds for the singlet case. The structure of the AP equations remains the same for the NLLA, with homogeneous and inhomogeneous parts. The solution of the homogeneous part, called the hadronic solution for its similarity to the nucleon case, has a term like in equation (2.34), only now the anomalous dimensions have to be calculated to second order, and also some nonlogarithmic contributions appear. The solution of the inhomogeneous part has now an additional term as compared to the LLA case:

$$f_\gamma(x,Q^2)|_{asymp} = \frac{4\pi}{\alpha_s(Q^2)}A(x) + B(x) \tag{2.47}$$

This is the asymptotic point–like solution in NLLA. The general solution of the AP equation, derived for the non–singlet case in the $\overline{MS}$ scheme and expressed in terms of moments, has the following form:

$$f^n_\gamma(Q^2) = \{f^{n0}_\gamma(Q^2_0)r^{-d^n_{qq}} + \frac{4\pi}{\alpha_S}\frac{a^n}{1-d^n_{qq}}(1-r^{1-d^n_{qq}}) + \frac{b^n}{d^n_{qq}}(1-r^{d^n_{qq}}) + O(\alpha_S)\} \tag{2.48}$$

with $r \equiv \frac{\alpha_S(Q^2)}{\alpha_S(Q^2_0)}$, and $f^{n0}_\gamma(Q^2_0)$ is related to the boundary condition imposed on the unknown hadronic component at an arbitrary Q^2_0 scale as in LLA. The coefficient d^n_{qq} is proportional

to the one loop anomalous dimension as in equation (2.35). The coefficients a^n and b^n are the n–th moments of $A(x)$ and $B(x)$

$$A^n = a^n/(1 - d^n_{qq}) \qquad (2.49)$$

$$B^n = b^n/d^n_{qq},$$

and can be calculated in perturbative QCD after inserting them into the evolution equations. The second and third terms in the brackets multiplying a^n and b^n in equation (2.48) arise, as in the LLA case, from the boundary condition related to the hadronic contribution. In the asymptotic limit of the full solution (eq. (2.48)) terms proportional to r drop out and one obtains an absolute NLLA prediction for the parton distributions in the photon, since now the results depend neither on the unknown hadronic components at Q_0^2 nor on Q_0^2.

A similar formula holds for the singlet case with its own moments. As it happens, the singularity problem for the singlet parton distributions becomes worse in NLLA than in LLA. Now, both the singlet A^n and B^n are singular and the singularity of B^n for $n = 2$ is such that in x–space $B(x) \sim x^{-2}$ and is negative for $x \sim 0$. As a result , the singlet parton distributions are singular and negative at small x. The situation is expected to get worse with each order of the calculation [27]. The consequences of this problem are seen already at moderate values of Q^2 where the calculated F_2^γ in NLLA remains negative up to x as large as 0.2 [28,19]. The problem will not disappear if the asymptotic solution is supplemented just by a finite VDM–like hadronic solution.

Since the structure function is a physical measurable quantity which cannot be negative, it becomes clear that the separation of the structure function into an asymptotic point–like contribution and a finite hadron–like contribution gives unphysical results. Thus, the hadronic contribution to the full NLLA solution cannot be discarded since its role is to cancel the singularity of the asymptotic solution but then one looses the absolute predictive power for the photon structure function in QCD.

The asymptotic solution in NLLA has also a singularity at $x = 1$. The situation is similar [26] to that at small x and will not be discussed here, especially since it is less important from the phenomenological point of view. For the sake of completeness, it should also be noted that the full NLLA prediction for F_2^γ contains a term which remains scheme dependent. The presence of this term for a physical quantity is due to the problem mentioned earlier, that some of the terms in the calculation are in fact of next-next-to-leading accuracy but not all contributions of this order are present in the NLLA approach. It was found that this contribution is small in the $\overline{MS}$ and the MOM schemes. Moreover, the NLLA prediction for F_2^γ retains a dependence on the boundary condition at Q_0^2. A detailed discussion of those aspects can be found in [19].

To save at least partly the uniqueness of the structure of the photon as a testing ground of QCD several approaches have been proposed. These are regularization schemes based either on the singularity cancellation between the point–like and hadron–like photon sectors [25] or on the regularization of the singularities in both sectors separately [29]. This approach necessitates the introduction of some phenomenological arbitrary parameters and it is not evident how this procedure affects the definition of parton distribution functions.

Thus, at the moment, the only consistent way to obtain physical results for the parton distributions of the photon and F_2^γ, is by solving the evolution equation with an experimental input at some scale Q_0^2, which takes into account the nonperturbative aspect of the structure of the photon.

2.3 Experimental extraction of F_2^γ

The photon structure function has been measured so far mainly with two e^+e^- machines: at PETRA and at PEP. Recently a measurement from TRISTAN has become available [30]. Three experiments have published the results of their measurements at PETRA: PLUTO [31], for average Q^2 values of 2.4, 4.3, 5.3, 9.2, and 45 GeV^2, TASSO [32], at $< Q^2 >$=23 GeV^2, and JADE [33] for $< Q^2 >$=24 and 100 GeV^2. Preliminary results exist for the CELLO detector for Q^2 values of 7, 13.1 and 28.8 GeV^2 [34]. At PEP, the TPC/2γ [35] group measured F_2^γ at $< Q^2 >$=0.24, 0.38, 0.71, 1.31, 2.83, 5.09, and 20 GeV^2. At TRISTAN the photon structure function has been measured by the AMY [30] group for $< Q^2 >$=73 GeV^2.

It is not easy to measure F_2^γ. In principle one needs measurements of Q^2 and x. By tagging the electron one determines the value of Q^2. This can be obtained with a precision in the range $\triangle Q^2/Q^2 \sim$ 7-10%, depending on the energy and angular resolution of the detector.

In order to obtain x, one needs a good measurement of the total hadronic energy W, which together with Q^2 yields x. However, due to finite resolution and limited acceptance of the detectors, one measures W_{vis}, the visible hadronic energy, which is usually smaller than W, and therefore the calculated x_{vis} from W_{vis} is larger than the true x of the event. One needs, thus, to unfold the true result from the visible measurement. This procedure needs a Monte Carlo program having a good simulation of the detector and a good description of the structure of the events. It depends on the fragmentation model used to generate the final state particles. In order to describe properly the measurable distributions, one usually needs to have a mixture of isotropic phase space and limited p_T phase space. Unfortunately, different experiments use different procedures, which makes the consistency checks between different experiments more difficult.

So far the statistics is quite limited. This causes either the data to be summed in large x bins or in large Q^2 bins or in both large x and large Q^2 bins. In order to be able to compare with theory at a specific value of Q^2, one has to assume a certain form factor [36,37] to extrapolate from the measured Q^2 to the quoted Q^2 value. That is the reason why the systematic errors are larger or of the same order as the statistical ones.

2.4 Parametrizations of parton distributions in the photon

The existing parametrizations of the photon structure function, all of LLA character, can be subdivided into two kinds. The first ones use the approach that the photon structure function can be indeed decomposed into a point–like part and a hadron–like part:

$$F_2^\gamma(x,Q^2) = F_2^{\gamma,PL}(x,Q^2) + F_2^{\gamma,HAD}(x,Q^2)$$

They differ among themselves by assuming different parametrizations for the point-like and the hadron-like contributions. In the second approach, no distinction is made between the point-like and the hadron-like contributions to the structure function and a parametrization, fixed at a given Q_0^2, is evolved to a different Q^2 through the AP equations.

In the first approach the point-like part is usually assumed to be given either by the QPM expression (see eq. (2.14)) or by the asymptotic LLA calculation. In the latter case, a convenient parametrization has been provided by Duke and Owens (DO) [28]. The relative strength of this point-like contribution depends on the value of the free parameters used in the calculation (quark masses or the scale parameter Λ). The separation into individual quark distributions follows naturally from the definition (2.15). The parametrizations of the hadron-like contribution are based mostly on the VDM approach, in which $F_2^{\gamma,HAD}(x,Q^2)$ is related to the vector meson structure functions F_2^V. Through isospin invariance the different F_2^V are expressed in terms of the only experimentally available mesonic structure function, that of the π^-, $F_2^{\pi^-}$. This last structure function is measured in the Drell-Yan reaction $\pi^- p \to \mu^+\mu^- X$ [38]. The result used most commonly

$$(F_2^{\gamma,HAD})_{VDM} = 0.2\alpha(1-x) \tag{2.50}$$

is called the standard VDM hadron contribution, and is in agreement with what one expects from counting rules for a bound $q\bar{q}$ system. There are more elaborate parametrizations of the π^- structure function, which therefore also give different forms for the VDM hadronic contribution. Owens and Reya (OR) [39] propose the form

$$F_2^{\gamma,HAD} = 0.42\sqrt{x}(1-x) + 0.11(1-x)^5, \tag{2.51}$$

while Castorina and Donnachie (CD) [40] have recently used

$$F_2^{\gamma,HAD} = 0.31\sqrt{x}(1-x)^{0.6} + 0.11(1-x)^5. \tag{2.52}$$

The OR parametrization of the hadron-like contribution has been used by Drees and Godbole [41] in their parametrization of the photon structure function, where the point-like part is taken as suggested by DO, with $\Lambda = 0.4$ GeV. Under additional assumptions concerning the separation into valence and sea contributions and the quark content of those, the VDM hadron-like parametrizations can be separated into individual quark distributions. The gluons have to be included in addition, with constraints coming from counting rules and momentum sum rules. This concerns only the gluons from the hadron-like contribution since in the photon case momentum sum rules do not apply in general. It should be noted that there is considerable freedom in the choice of the sea quark and gluon distributions.

The approach through evolution equations of the structure function has been undertaken by Drees and Grassie (DG) [42]. They used the LLA modified AP equations to evolve an input parametrization of parton distributions at $Q_0^2 = 1$ GeV^2 so that it fits the PLUTO data [43] at 5.9 GeV^2. They start at the input with 3 flavors and evolve to higher Q^2 using 4 and 5 flavors. For Λ they assume a value of 0.4 GeV. The advantage of this approach is that there is no worry about possible double counting [44] when adding the point-like and the hadron-like parts. It is free of divergences induced by the asymptotic point-like solution as the one of DO at $x \to 0$. Although in this approach, the gluon distribution could be part

of the fit, the data available at that time were too sparse to attempt such a fit. The same procedure has recently been applied to all existing data on the photon structure function and a new parametrization, this time including a fit to the gluon distribution, has been obtained by Abramowicz, Charchula and Levy (LAC) [45]. The evolution is carried out for four flavors with a Λ value assumed to be 0.2 GeV. The parametrization is provided for different starting values of Q_0^2, ranging from 1 to 4 GeV^2. It has been checked that the results do not depend on the value of Q_0^2 for $Q_0^2 > 2$ GeV^2, although the data are well reproduced for all starting values.

There is also a class of parametrizations of the photon structure function which does not provide parton distributions [25,29,46], but a detailed discussion of those is outside the scope of this paper.

It is worthwhile to notice that in all the parametrizations in which the hadron-like contribution is described by VDM, $F_2^{\gamma,HAD}$ is Q^2 independent. In that respect the only parametrization, not based on the AP evolution equations, which has a Q^2 dependence of $F_2^{\gamma,HAD}$ built in naturally is the one by Gotsman, Levy and Maor [46] (GLM), based on a Regge type of approach.

The comparison of the most popular parametrizations of F_2^γ with the data is presented in figure 12. In order to follow the traditional presentation of the proton structure functions, the comparison is shown as a function of Q^2 for different x bins. The data show a clear positive scale breaking for all x values. The data are best reproduced by the DG and GLM parametrizations, although at low Q^2 the data lie below the curves. The parametrizations based on a VDM-like hadronic contribution predict too high values in the low x region. All the parametrizations describe well the large x region, dominated by the point-like contribution.

A more detailed comparison of the new LAC parametrizations ($Q_0^2 = 1$ and 4) with the data, together with the DG predictions is shown in figure 13a,b. This time the comparison is made in fixed Q^2 bins as a function of x and spans all the available data above the lowest starting value used for the LAC and DG parametrizations, $Q^2 = 1$ GeV^2. In general, above $Q^2 = 5$ GeV^2 both the LAC and DG parametrizations reproduce the data quite well. Below that Q^2, the LAC parametrization starting at $Q_0^2 = 1$ GeV^2 gives a better description of the data. It should be kept in mind though that at the time when the DG parametrization was determined only preliminary PLUTO data at $Q^2 = 5.9$ GeV^2 were available. The basic difference between the DG parametrization and the LAC one which starts at $Q_0^2 = 4$ GeV^2 is in the very low x region, where the LAC parametrization predicts a sharp rise of the structure function. The comparison between the predictions for the u quark distribution in the photon, for the DO, DG and the LAC parametrizations is shown as a functions of Q^2 for fixed values of x in figure 14 and as a function of x for fixed Q^2 in figure 15. The spread of various predictions for the u quarks is of the same order as the one for F_2^γ and reflects the inherent uncertainty in the data. A comparison of the gluon distributions obtained in the LAC parametrizations for various starting values of Q^2 and that assumed in the DG one, evolved to $Q^2 = 10$ and 50 GeV^2 is presented in figure 16. It is clear from this comparison that although the data seem to be able to accommodate more gluons than was assumed by DG, there is quite a lot of freedom in the choice of the gluon distribution in the photon. It should also be noted that the gluon distribution obtained for the LAC parametrization with the initial value of $Q^2 = 1$ GeV^2 has an unusual shape which peaks at high x and which is difficult to understand.

Chapter 3

Structure of virtual photons

So far the discussion was limited to the structure of real or quasi–real photons. The natural question that one is faced with is what happens to a virtual photon and whether it is legitimate to think that in DIS of charged leptons on nucleons it is indeed the structure of the nucleon that is probed and not some kind of convolution of both the structure of the target and of the probe. The same question could be asked in the case of the DIS $e\gamma$ scattering.

As in the case of the quasi–real photon, the structure of the virtual photon can be introduced through cross section considerations and, if so, the structure of the virtual photon can be probed in e^+e^- two photon collisions, by requiring double tagged events, in which both the probing and the probed photons are virtual. This goal is not easy to attain as the rates for double–tag photon–photon reactions is considerably smaller than for single–tag rates [5]. From the theoretical point of view, there are two scales involved for the virtual photon: the virtuality of the probe q^2, such that $q^2 = -Q^2 < 0$ and the virtuality of the target photon p^2, such that $p^2 = -P^2 < 0$.

$F_2^{\gamma^*}$ can be calculated in the Parton Model from the box diagram. Following the procedure applied to the real photon case, one can define the quark distributions in the virtual photon via relation (2.15). The Parton Model result obtained under the assumption that

$$\Lambda^2 \ll P^2 \ll Q^2, \tag{3.1}$$

where $\Lambda \equiv \Lambda_{QCD}$, is the following [48]:

$$q_{i,QPM}^{\gamma}(x,Q^2) = \frac{N_c\alpha}{2\pi}e_{q_i}^2\,[x^2+(1-x)^2]\ln\frac{Q^2}{P^2} + \text{finite constant terms.} \tag{3.2}$$

Condition (3.1) allows to neglect in (3.2) terms proportional to P^2/Q^2, Λ^2/Q^2, and Λ^2/P^2. The leading logarithmic term corresponds to the logarithm of the ratio of two virtualities and there is no need for terms dependent on Λ, which were present in the case of massless quarks. Note that if in formula (3.2) P^2 is substituted by Λ^2, one obtains the result for the real photon.

For $P^2 \sim Q^2$ this leading logarithmic contribution vanishes. That leads to the structureless nature of a highly virtual photon, where highly virtual means that the photon has the highest virtuality characteristic for a given process.

The structure of a virtual photon, in the limit (3.1) has been studied by Uematsu and Walsh [48]. The result obtained in the NLL approximation for the non–singlet case is:

$$f_{\gamma^*}^n(Q^2,P^2) = \frac{4\pi}{\alpha_S}\frac{a^n}{1-d_{qq}^n}(1-\rho^{1-d_{qq}^n}) + \frac{b^n}{d_{qq}^n}(1-\rho^{d_{qq}^n}) \tag{3.3}$$

with $\rho \equiv \alpha_S(Q^2)/\alpha_S(P^2)$, and all the other quantities are defined as for the real photon case (2.48). Here the hadronic part which is expected to behave like $1/P^2$ has been neglected [48]. Note the similarity and the differences between expression (3.3) and that for the real photon (2.48). The above formula contains the asymptotic solution regularized by terms calculable in QCD containing two physical scales Q^2 and P^2. Therefore, the above expression is finite and can be used as an absolute prediction of QCD without an arbitrary scale Q_0^2 which appears in the relevant solution for the real photon (and which is a reminder of the non–perturbative contribution to the real photon structure function).

The importance of the virtual photon structure function in obtaining the scale parameter Λ_{QCD} is discussed in [49]. It is shown that this scale can be determined reliably once all available theoretical and experimental information concerning both the real and the virtual photon are exploited.

There is no prescription as yet how to use the notion of the structure function of the virtual photon in practical applications as those related to the study of the physics potential at HERA, where some of the reactions of interest are indeed initiated by virtual photons. Part of the problem lies in the definition of the flux of virtual particles. As it is, since the virtuality of the photons which dominate the cross section is small, one is left with the one photon approximation which does work in this regime.

Additional progress on the issue of the virtual photon is clearly needed and will become essential for a more elaborate analysis of HERA results, soon to come.

Chapter 4

The role of the photon structure function at HERA

As stated in the introduction, a large portion of the ep interactions will be in the Q^2 region where the photon from the incoming electron is almost real. These are the "photoproduction" events, which will be studied at HERA at a "γp" c.m. energy which is an order of magnitude higher than the presently available ones (on average $\sim$ 200 GeV).

Although in many hard photoproduction reactions the dominant contribution comes from processes in which the photon acts as a direct photon, there are some reactions in which the resolved photon plays an important role. The predictions for these latter reactions depend therefore on the parton distributions of the photon, and, thus, provide a way to "measure" them.

Three methods have been proposed so far for the determination of the parton distributions of the photon: two jet production, J/Ψ production and deep inelastic Compton scattering.

4.1 Two jet production

The two jet cross section of events produced at HERA has been studied by Drees and Godbole [21]. It was found that for jets with $p_T \leq 40$ GeV the cross section is dominated by the resolved photon contribution. This contribution, and in particular the one that is initiated by a gluon coming from the photon, is especially important at large jet rapidities. Using the DG [42] and the DO [28] parametrizations of the partons in the photon they show that the contribution from the quark and gluon content of the photon actually dominates the two jet cross section at HERA for p_T up to 40 GeV, and contributes about 20% to the total $b\bar{b}$ and $c\bar{c}$ cross sections.

4.2 J/Ψ "photoproduction"

It has been suggested by Fletcher, Halzen and Robinett [50] that the subprocess $\gamma g \to J/\Psi g$ could be used to probe the gluon structure of the photon. The direct and the resolved photon

contribution to the reaction compete for low p_T's of the produced J/Ψ but the ones produced at high rapidity are induced mainly by the resolved photon contribution and can be used to isolate it. The same should hold also for χ "photoproduction" at HERA, which through the decay $\chi \to J/\Psi\gamma$, would be another source of J/Ψ production.

4.3 Deep inelastic Compton scattering (DIC)

The inclusive photoproduction process of deep inelastic Compton scattering $\gamma p \to \gamma X$, in which photons with transverse momenta $p_T^\gamma \geq 5$ GeV are produced has been studied by Aurenche et al. and by Bawa, Krawczyk and Stirling [51] for the HERA domain. It has been shown that the QED Compton scattering can be used to study the quark and gluon distributions both in the photon and in the proton in the region 5 GeV$\leq p_T^\gamma \leq$15 GeV.

Acknowledgments

We are indebted to M.Drees from DESY for useful discussions and a very careful and critical reading of this manuscript. We would like to acknowledge helpful discussions with S.Pokorski, B.Badełek from Warsaw University, E.Gotsman from Tel-Aviv University, G.Wolf from DESY, R.Godbole from University of Bombay, and E.M.Levin from the Leningrad Nuclear Physics Institute. Three of us (HA, KCh and MK) acknowledge the support of the Polish Government and Ministry of Education Research Programs CPBP 01.03, 01.06 and GMEN 133/90 as well as the DESY Directorate for supporting their visits at DESY. One of us (HA) would like to thank the Alexander von Humboldt Stiftung for supporting her stay at DESY. UM would like to thank the Minerva Foundation for the financial support which made his stay at DESY possible. This work was also partly supported by the German Israeli Foundation (GIF I–149–110.7/89).

Bibliography

[1] C.F.Weizsäcker, Z. Phys. 88, 612 (1934); E.J.Williams, Phys. Rev. 45, 729 (1934).

[2] P.Kessler, Nouvo Cimento 17, 809 (1960).

[3] J.H.Field, VIIIth International Workshop on Photon–Photon Collisions, Shoresh, Jerusalem Hills Israel, 1988.

[4] U.Maor, Acta Phys. Polonica B19, 623 (1988).

[5] Ch.Berger, W.Wagner, Phys. Rep. 146, 1 (1987).

[6] T.H.Bauer et al., Rev. Mod. Phys. 50, 261 (1978).

[7] J.J.Sakurai, Ann. Phys. 11, 1 (1960).

[8] J.J.Sakurai, D.Schildknecht, Phys. Lett. 40B, 121 (1972).

[9] M. Greco, Nucl. Phys. B63, 398(1973).

[10] V.M.Budnev et al., Phys. Rep. 15C, 181 (1975).

[11] C.G.Callan, D.J.Gross, Phys. Rev. Lett. 22, 156 (1969).

[12] E.Witten, Nucl. Phys. B120, 189 (1977).

[13] W.A.Bardeen, A.J.Buras, Phys. Rev. D20, 166 (1979); Phys. Rev. D21, 2041 (1980).

[14] C.H.Llewellyn Smith, Phys. Lett. 79B, 83 (1978); W.R.Frazer, J.F.Gunion, Phys. Rev. D20, 147 (1979).

[15] G.Altarelli, G.Parisi, Nucl. Phys. B126, 298 (1977); L.N.Lipatov, Sov. J. Nucl. Phys. 20, 94 (1975).

[16] R.J.De Witt et al., Phys. Rev. D19, 2046 (1979); Phys. Rev. D20, 1751 (1979).

[17] C. Peterson, T.F.Walsh, P.M.Zerwas, Nucl. Phys. B229, 301 (1983).

[18] M.Glück, E.Reya, Phys. Rev. D28, 2749 (1983).

[19] M.Glück, K.Grassie, E.Reya, Phys. Rev. D30, 1447 (1984).

[20] A.C.Bawa, W.J.Stirling, J. Phys. G: Nucl. Phys. 15, 1339 (1989).

[21] M.Drees, R.M.Godbole, Phys. Rev. D39, 169 (1989).

[22] J.R.Cudell, F.Halzen, C.S.Kim, Int. J. Mod. Phys. A3, 1051 (1988).

[23] G.'t Hooft, M.Veltman, Gauge Theory of Weak and Electromagnetic Interactions, p. 322, ed. C.H.Lai, 1982 and references therein.

[24] G.Altarelli, Phys. Rep. 81, 1 (1982).

[25] I.Antoniadis, G.Grunberg, Nucl. Phys. B213, 445 (1983).

[26] W.R.Frazer, G.Rossi, Phys. Rev. D25, 843 (1982).

[27] G.Rossi, Phys. Rev. D29, 852 (1984).

[28] D.W.Duke, J.F.Owens, Phys. Rev. D26, 1600 (1982).

[29] J.H.Field, F.Kapusta, L.Poggioli, Phys. Lett. 181B, 362 (1986); Z. Phys. C36, 121 (1987).

[30] AMY Coll., T.Sasaki et al., Phys. Lett. 252B, 491 (1990).

[31] PLUTO Coll., Ch.Berger et al., Z. Phys. C26, 353 (1984); Phys. Lett. 142B, 111 (1984); Phys. Lett. 149B, 421 (1984); Nucl. Phys. B281, 365 (1987).

[32] TASSO Coll., H.Althoff et al., Z. Phys. C31, 527 (1986).

[33] JADE Coll., W.Bartel et al., Z. Phys. C24, 231 (1984).

[34] CELLO Coll., H.J.Behrend et al., contributed to the XXVth International Conference on HEP, Singapore 1990.

[35] TPC/2γ Coll., D.Bintiger et al., Phys. Rev. Lett. 54, 763 (1985); H.Aihara et al., Phys. Rev. Lett. 58, 97 (1987); Z. Phys. C34, 1 (1987).

[36] I.F.Ginzburg, V.G.Serbo, Phys. Lett. 109B, 231 (1982).

[37] U.Maor, E.Gotsman, Phys. Rev. D28, 2149 (1983).

[38] C.B.Newman et al., Phys. Rev. Lett. 42, 951 (1979).

[39] J.F.Owens ,E.Reya, Phys. Rev. D17, 3003 (1978).

[40] P.Castorina, A.Donnachie, Z. Phys. C45, 497 (1990).

[41] M.Drees, R.M.Godbole, Nucl. Phys. B339, 355 (1990).

[42] M.Drees, K.Grassie, Z. Phys. C28, 451 (1985).

[43] Ch.Berger, International Symposium on Lepton and Photon Interactions at High Energy, Cornell (1983).

[44] W.R.Frazer, Phys. Lett. 194B, 287 (1987).

[45] H.Abramowicz, K.Charchula, A.Levy, Submitted to the LP-HEP91 Conference, Geneva, 1991.

[46] E.Gotsman, A.Levy, U.Maor, Z. Phys. C40. 117 (1988).

[47] J.H.DaLuz Vieira, J.K.Storrow, Phys. Lett. 205B, 367 (1988).

[48] T.Uematsu, T.F.Walsh, Phys. Lett. 101B, 263 (1981); Nucl. Phys. B199, 93 (1982).

[49] W.Ibes, T.F.Walsh, UMN–TH–837/90.

[50] R.S.Fletcher, F.Halzen, R.W.Robinett, Phys. Lett. B225, 176 (1989).

[51] P.Aurenche et al., HERA Workshop 1987, p.561; M.Krawczyk, Acta Physica Polonica B21, 999 (1990); A.C.Bawa, M.Krawczyk, W.J.Stirling, Z. Phys. C50, 293 (1991); A.C.Bawa, M.Krawczyk, DESY 90–154 (to be published in Phys.Lett.B).

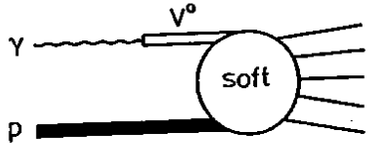

Figure 1: VDM diagram for $\gamma p \rightarrow$ hadrons.

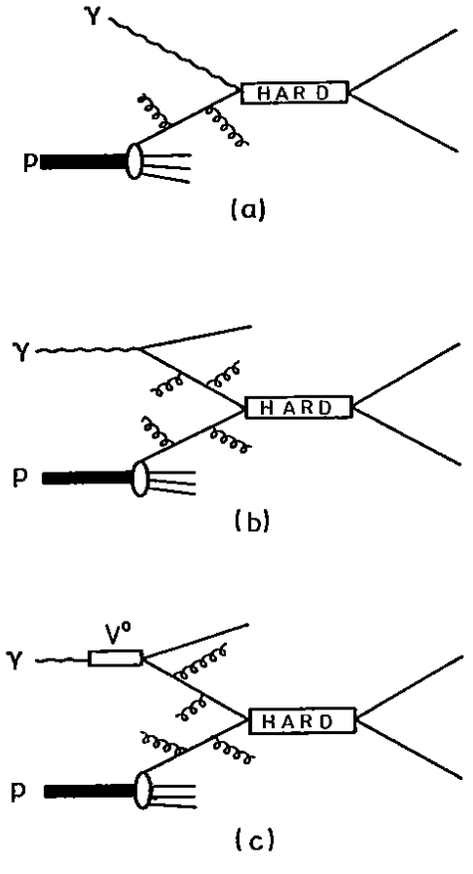

Figure 2: Diagrams for a γp hard process. a) A direct photon contribution to 2–jet production. b) The point–like contribution to the resolved photon contribution to 2–jet production. c) The hadron–like contribution to the resolved photon contribution to 2–jet production.

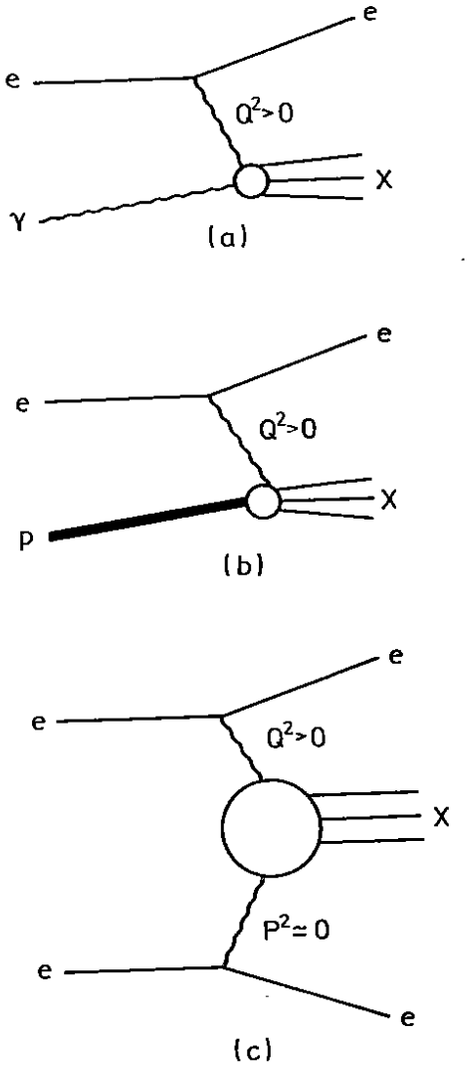

Figure 3: DIS diagrams:a) $e\gamma$ scattering, b) ep scattering, c) two–photon exchange in e^+e^- scattering.

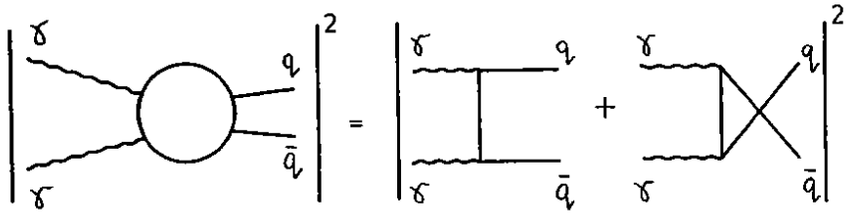

Figure 4: The diagramatic presentation of the cross section for the process $\gamma\gamma \to q\bar{q}$ in QPM.

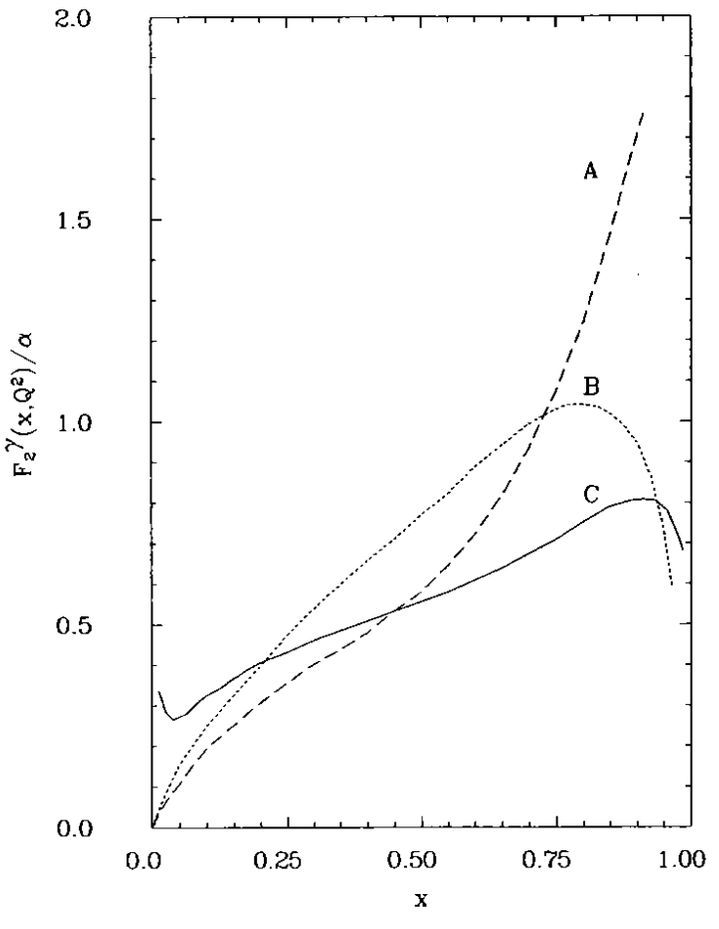

Figure 5: The prediction for the x dependence of F_2^γ as given in the leading log Q^2 approximation of the QPM (A), in the full QPM (B) and the LL QCD calculation (C).

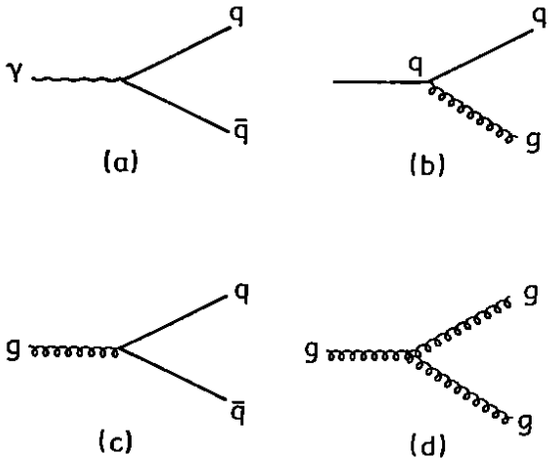

Figure 6: Splitting functions utilized in the AP equations. a) h_{box}, b) P_{qq} or P_{qG}, c) P_{Gq}, d) P_{GG}.

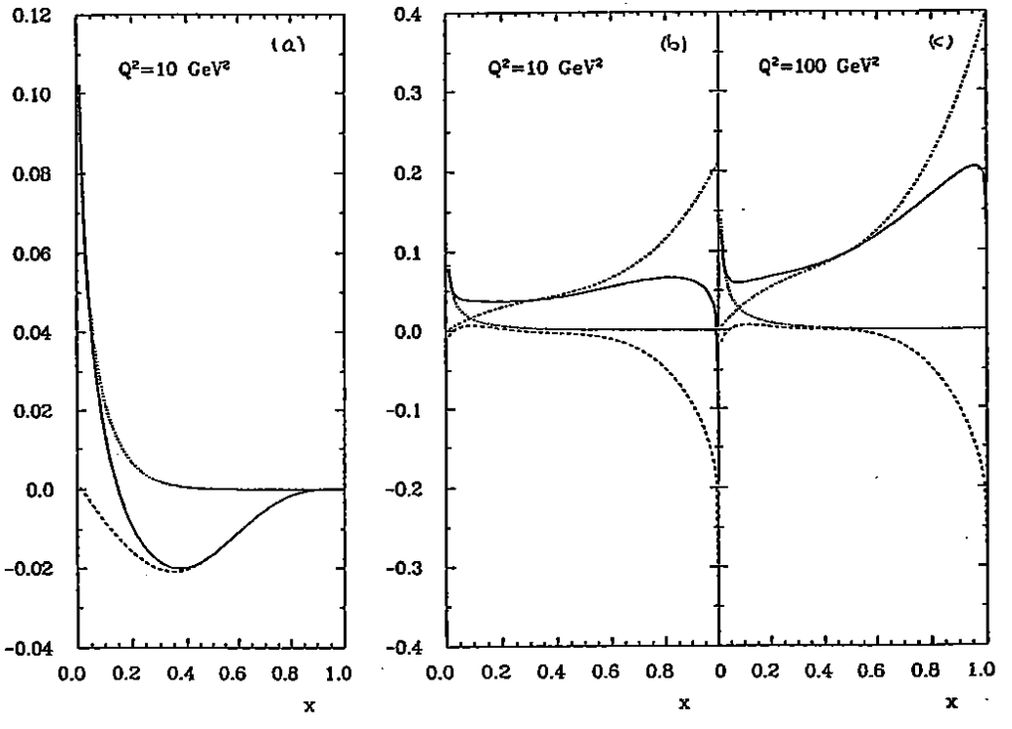

Figure 7: Contributions to the Q^2 evolution of F_2^p and F_2^γ. a) $dF_2^p/d\ln Q^2$ as a function of x shown for $Q^2 = 10$ GeV^2. The dotted line denotes the contribution from gluons emitting quarks (P_{qG} term), the dashed line denotes the contribution from quarks emitting quarks (P_{qq} term) and the full line is the superposition of both. $dF_2^\gamma/d\ln Q^2$ as a function of x for b) $Q^2 = 10$ GeV^2 and for $Q^2 = 100$ GeV^2. In addition to the gluon and quark contributions denoted as in a), the dashed–dotted line is the contribution coming from the box–diagram (h_{box}). The full line is a superposition of the three contributions.

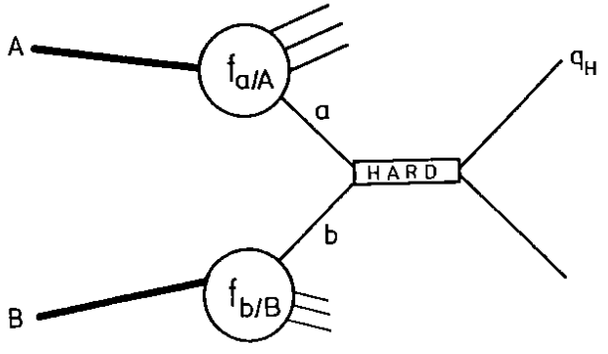

Figure 8: Diagram for the hard process $A + B \rightarrow q_H + X$.

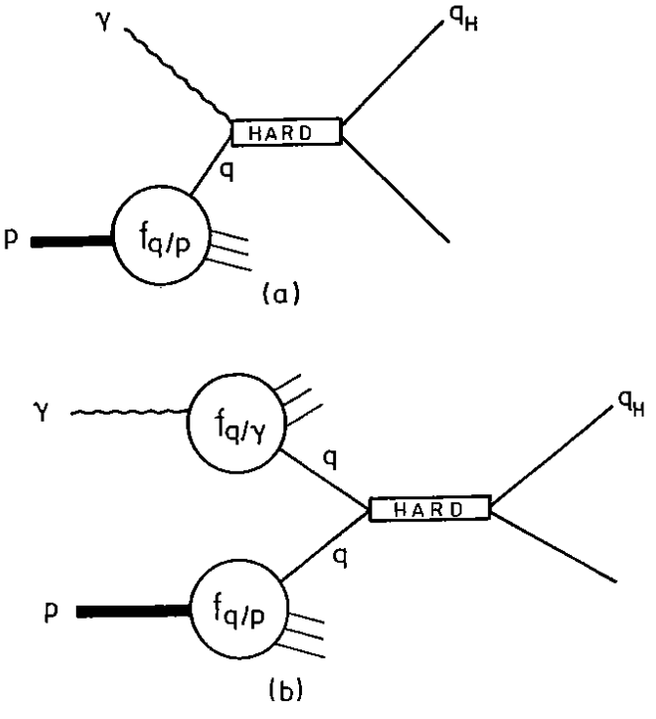

Figure 9: Diagram for the hard photoproduction process $\gamma + B \rightarrow q_H + X$. a) The direct photon contribution, b) the resolved photon contribution.

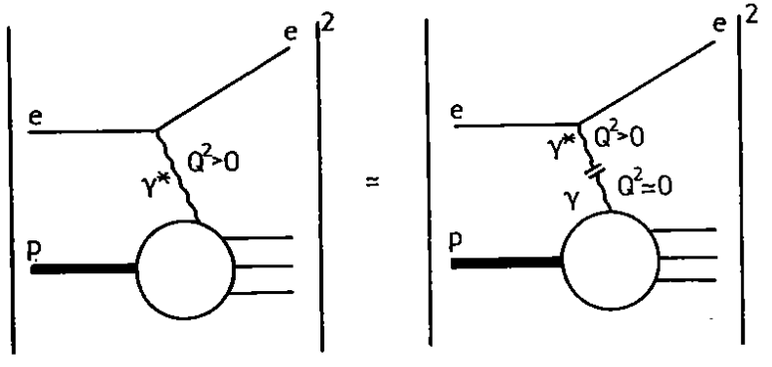

Figure 10: The one photon WW approximation for DIS of *ep*.

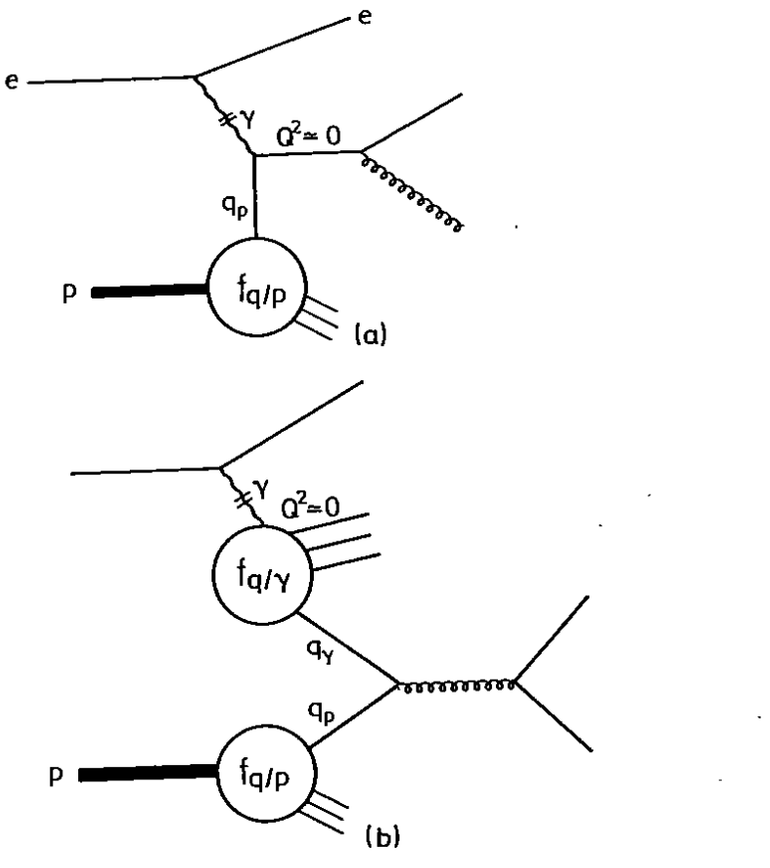

Figure 11: Diagrams for 2–jet production at HERA. a) The direct photon contribution, b) the resolved photon contribution.

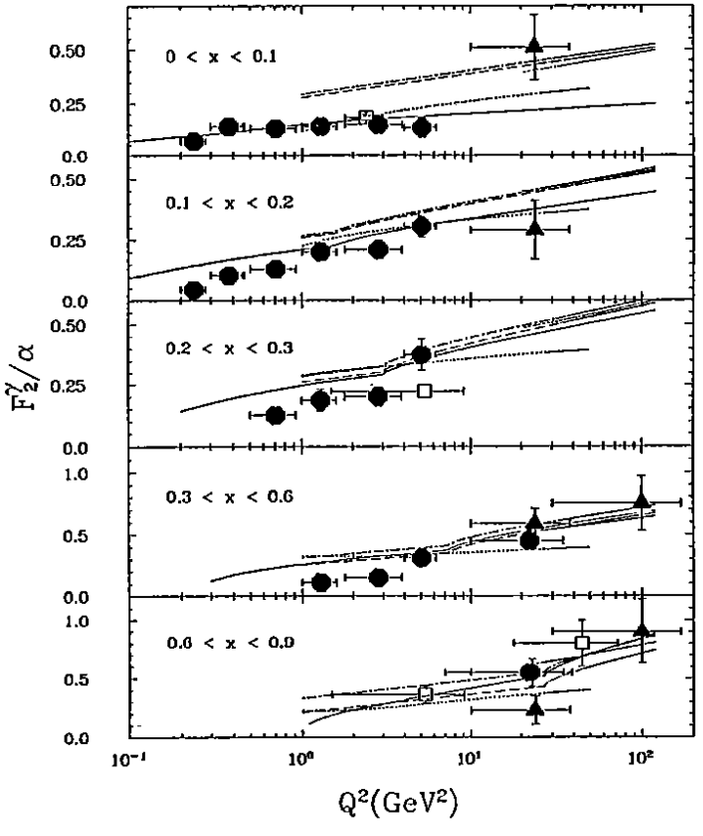

Figure 12: Comparison between the predictions of the parametrizations GLM (line), DG (dots), CD (dashes) and DGO (dash–dot) and F_2^γ data as function of Q^2, for different intervals in x. The data are from TPC (points), JADE (triangles) and PLUTO (squares)

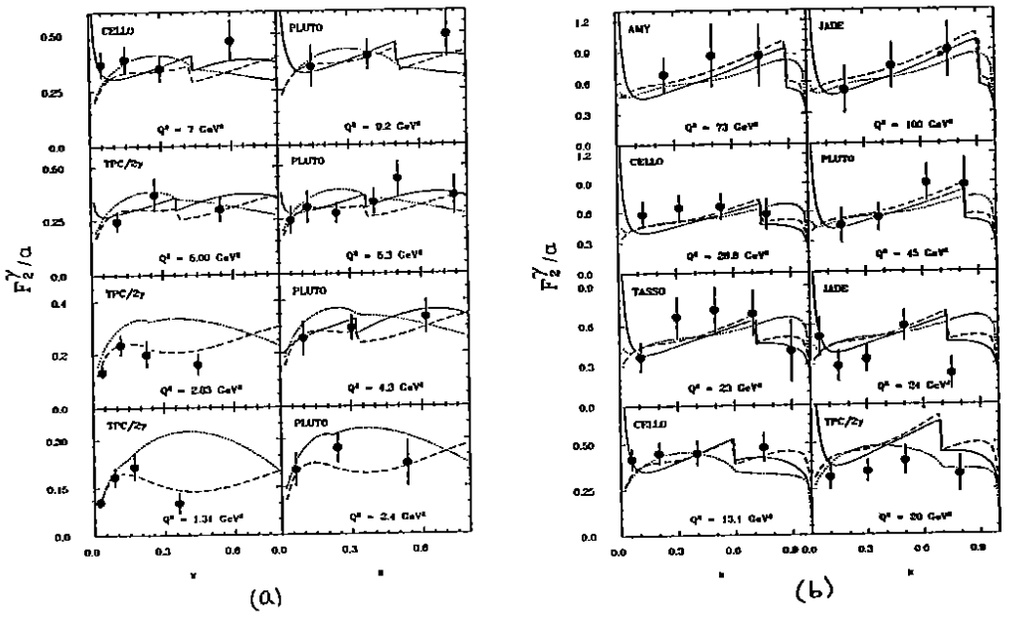

Figure 13: Comparison of the predictions of the LAC parametrization with $Q_0^2 = 1$ GeV^2 (dashed line), with $Q_0^2 = 4$ GeV^2 (full line) and the DG parametrization (dotted line) with the measurements of F_2^γ as a function of x in bins of Q^2. a) $1.31 < Q^2 < 9.2$ GeV^2, b)$13.1 < Q^2 < 100$ GeV^2.

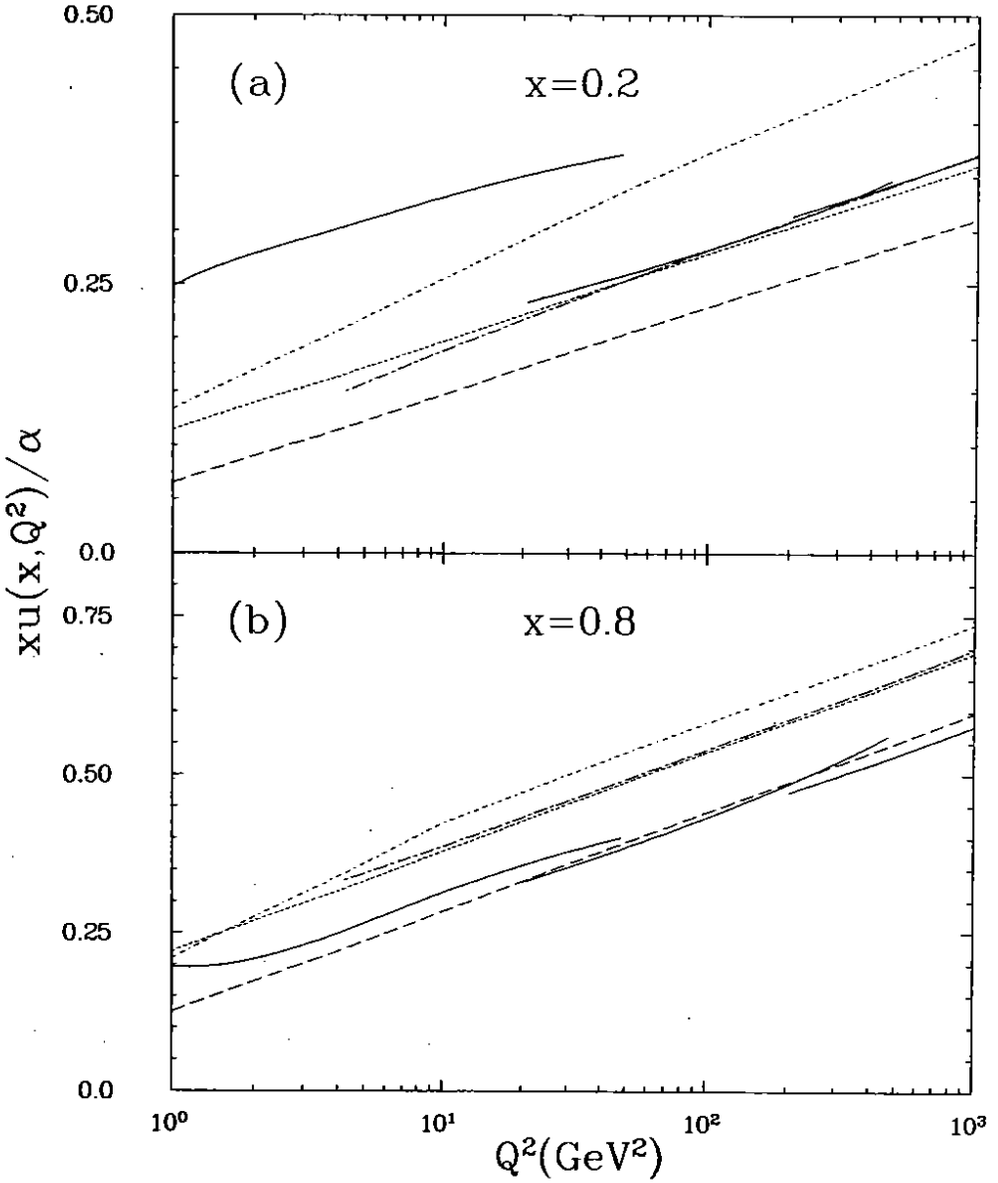

Figure 14: Comparison between the u quark distributions obtained for the DG parametrization ($\Lambda = 0.4$ GeV, full line), the DO parametrizations with $\Lambda = 0.2$ GeV (dotted line) and $\Lambda = 0.4$ GeV (dashed line), the LAC parametrizations with $Q_0^2 = 4$ GeV^2 ($\Lambda = 0.2$ GeV, dashed dotted line) and $Q_0^2 = 1$ GeV^2 ($\Lambda = 0.2$ GeV^2, double dashed dotted line) as a function of Q^2 for (a) $x = 0.2$ and (b) $x = 0.8$. (The discontinuity in the DG parametrization is due to a particular treatment of heavy flavours contribution to F_2^γ.)

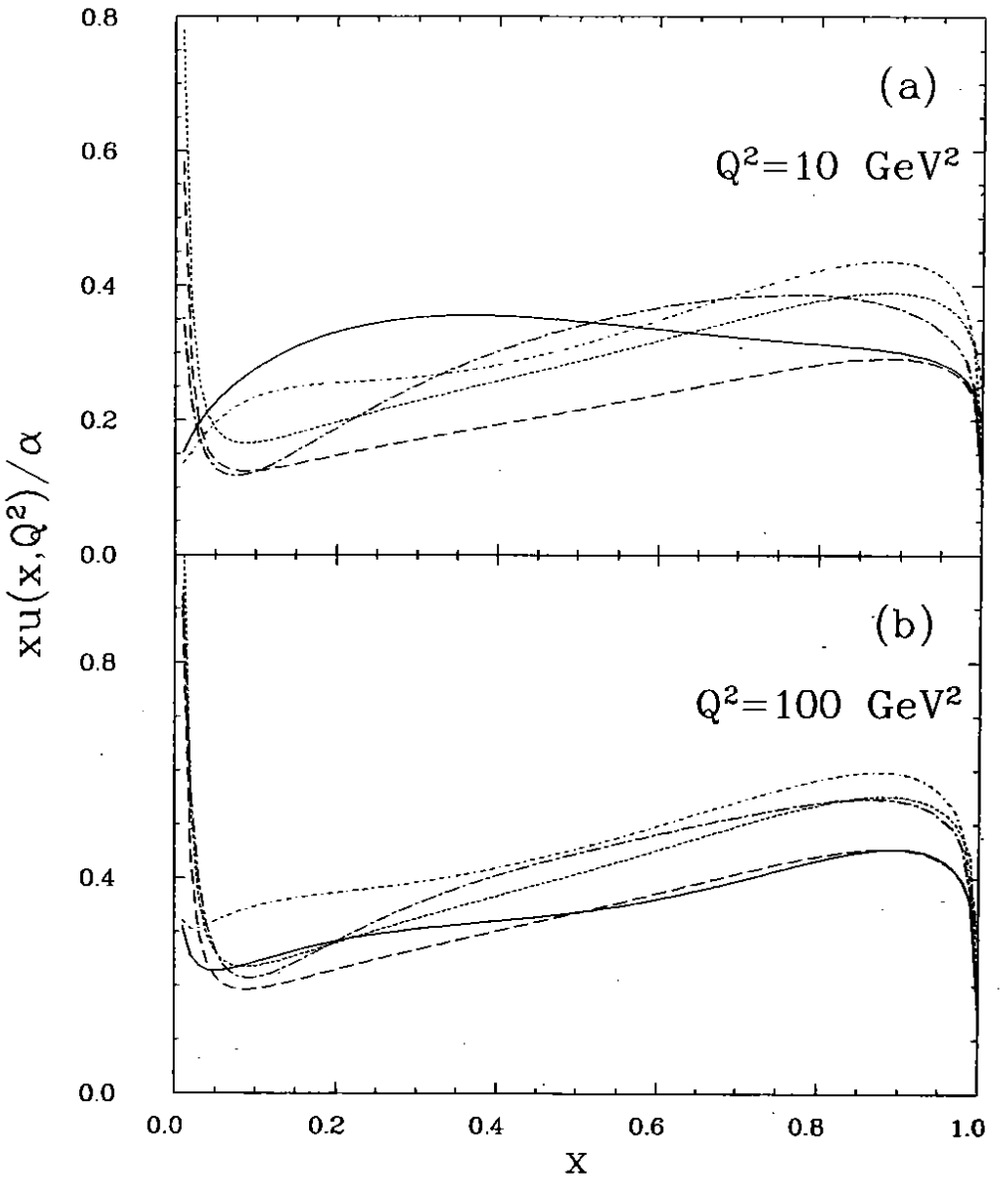

Figure 15: Comparison between the u quark distributions obtained for the DG parametrization ($\Lambda = 0.4$ GeV, full line), the DO parametrizations with $\Lambda = 0.2$ GeV (dotted line) and $\Lambda = 0.4$ GeV (dashed line), the LAC parametrizations with $Q_0^2 = 4$ GeV^2 ($\Lambda = 0.2$ GeV, dashed dotted line) and $Q_0^2 = 1$ GeV^2 ($\Lambda = 0.2$ GeV^2, double dashed dotted line) evolved to (a) $Q^2 = 10$ GeV^2 and (b) $Q^2 = 100$ GeV^2.

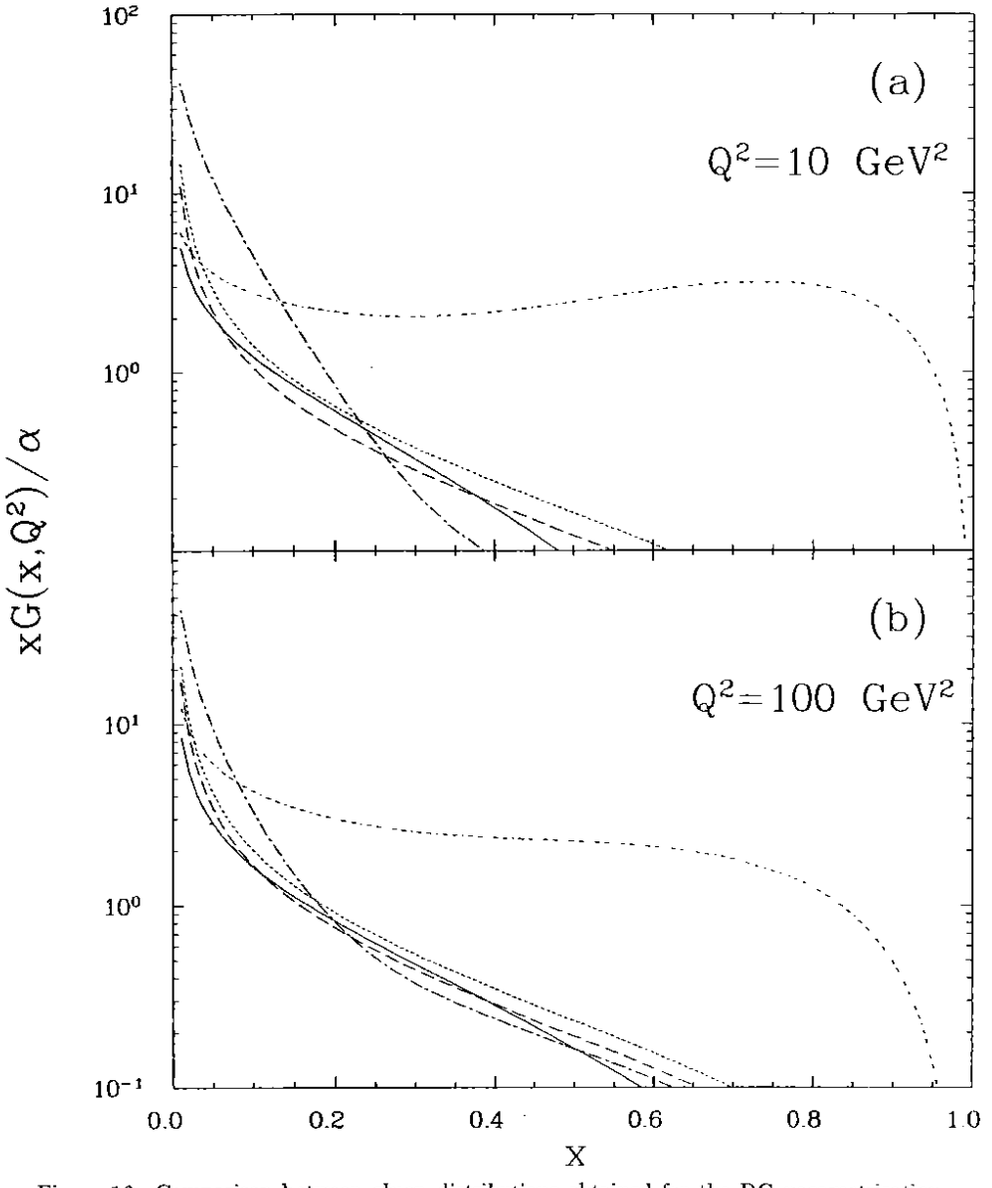

Figure 16: Comparison between gluon distributions obtained for the DG parametrization (Λ = 0.4 GeV, full line), the DO parametrizations with Λ = 0.2 GeV (dotted line) and Λ = 0.4 GeV (dashed line), the LAC parametrizations with Q_0^2 = 4 GeV^2 (Λ = 0.2 GeV, dashed dotted line) and Q_0^2 = 1 GeV^2 (Λ = 0.2 GeV^2, double dashed dotted line) evolved to (a) Q^2 = 10 GeV^2 and (b) Q^2 = 100 GeV^2.